# MINIATURIZED UNDERWATER FISHBONE – SLOT INTEGRATED PATCH ARRAY ANTENNA FOR FRESHWATER APPLICATIONS

NOR H. DAUD<sup>1</sup>, A. ISMAIL<sup>1,\*</sup>, A. SALI<sup>1</sup>, MOHD H. ISMAIL<sup>2</sup>

Wireless and Photonics Networks Research Centre, Department of Computer and Communication Systems Engineering Faculty of Engineering, Universiti Putra Malaysia, 43400, UPM Serdang, Selangor DE, Malaysia
 Department of Nature Parks and Recreation, Faculty of Forestry and Environment, Universiti Putra Malaysia, 43400, UPM Serdang, Selangor DE, Malaysia
 \*Corresponding Author: alyani@upm.edu.my

#### Abstract

The size restrictions present a significant issue when designing antennas for underwater applications that use electromagnetic (EM) waves for communication. Underwater antenna become complex and challenging to manufacture in addition to having bulk and weight issues. Additionally, it is impractical to establish wireless sensor networks underwater due to the high antenna size. To address this issue, this paper investigates and develops a proposed underwater antenna that consists of 1 × 2 linear Rectangular Microstrip Patch Array Antennas (RMPAAs) integrated with a fishbone-shaped slot and rounded corner based on a truncated ground plane and a T-shaped slot structure. The simulated results offered noteworthy compatibility with the measured results. The proposed antenna array has achieved better performance than other underwater antennas recently published in scientific journals in terms of return loss, bandwidth, and antenna dimensions. The antenna shows high performance, including an impedance bandwidth of 400 MHz (43.3%) at operating frequency of 921 MHz and a return loss magnitude of 30.0 dB (around 53.3%), especially in comparison to the previously reported designs of 14.0 dB. The overall dimensions of the proposed underwater antenna are 54 × 43 mm<sup>2</sup> with a finite ground plane of  $25 \times 43 \text{ mm}^2$ . Meanwhile, the total area of the proposed antenna was minimized by 2322 mm<sup>2</sup> (around 96.0%), especially in comparison to the previously reported designs of 58000 mm<sup>2</sup>. The findings indicate that the proposed underwater antenna is well suited for safety device applications. The critical challenges have also been identified and addressed in this research.

Keywords: EM wave propagation in freshwater, Rectangular patch array antennas, RF underwater communication, Sub-GHz frequency, Wideband.

#### 1. Introduction

Nowadays, the demand for small antennas operating at low frequencies is increasing [1]. However, there are many challenges for researchers to focus on while designing antennas. Scholars around the world have proposed a lot of minimization techniques in order to reduce the size of the antennas. A conventional way of reducing the size of a microstrip antenna is by employing a substrate material with a high value of dielectric constant and a thick dielectric substrate. But that approach is leading to high surface wave losses [2]. Changing the shape of the patch or introducing slots on the patch is a commonly used technique to miniaturize the Microstrip Patch Antenna (MPA) [3]. Numerous antennas that are intended for wearable applications have been proposed as a part of an underwater communications system, such as for safety devices. The smaller size of the antenna dimension is preferred to support miniaturized devices. However, the antenna dimension is inversely proportional to the working frequency. The lower the working frequency, the greater the antenna size [4].

Recently, the increasing demand for current human freshwater activities, such as water sports, encouraged the researchers to explore this study in an alternative approach. Natural waterways, such as rivers, are frequently drowning sites, in accordance with factors found in the literature. The primary cause of the unexpected accidents that happened to the visitors is thought to be a general lack of public knowledge on water safety. Rescue teams arriving at a scene of an accident have limited time for search work to help the victims. The actual response times for search and rescue are influenced by a number of unexpected factors, such as the distance of the vehicle from the accident site, traffic density, geographical factors, or weather conditions. Experience has also shown that application-trained dogs are not universally capable of working under any conditions. For this rescue operation to be done efficiently, they must have a smart device that can be used to detect the presence of a live person in a place of search.

Therefore, this study aims to design an underwater antenna that can be used as a safety device that can later be used as an emergency alert system. Besides, the main contribution of this work is to propose a method for enhancing the performance of miniaturized RMPAAs loaded with several miniaturization methods as well as a method to enhance the antenna bandwidth and return loss.

#### 2. Related Works

In this section, a review of the related work is presented. Freshwater is considered a medium that has low losses due to its low conductivity [5]. Recently, various types of antennas have been tested for freshwater applications in the sub-GHz frequency region. The previous research by Abdou et al. [6] explored a research study based on designing a bowtie antenna and testing it in air and water without a matching circuit. Meanwhile, a research study by O'Keefe and Perhirin [7] investigated the possibility of using Planar Inverted F Antenna (PIFA), but the proposed design only mentioned the measured bandwidth without considering the simulation parts, both in air and water conditions. Few other authors have presented work on buffer layers to improve antenna performance when operating underwater. Work done by Mohd Zali et al. [8] introduced a conventional wideband circular patch antenna integrated with an optimised buffer layer structure at 250 MHz.

However, the antenna dimensions are too large and not practical for the actual application in reality.

Other research undertaken by Dala and Arslan [9] has also proposed a novel approach to antenna design to study the feasibility of using the long-range (LoRa) 868 MHz frequency in underwater and water-surface communication. The authors enhanced its bandwidth by incorporating an oil-impregnated paper barrier around the FR4 material antenna with a total dimension of 8400 mm². Nevertheless, the dimensions of the antenna are still large. Another study conducted by Jaafar et al. [10] studies the effect of the physical parameters of water on the helical antenna's performance when the antenna operates in a water environment, but there is no measurement of the bandwidth of the antenna.

However, there are few studies that focus on the miniaturization of underwater antennas for consideration of applications in reality. In this regard, a proposed  $1\times 2$  linear RMPAAs integrated with a fishbone-shaped slot and rounded corner based on a truncated ground plane and T-shaped slot structure is designed and presented. The proposed underwater antenna is carefully designed to meet the specifications of sub-GHz frequency at 921 MHz operating mode. The performance of the proposed antenna is measured in terms of antenna dimensions, return loss magnitude,  $S_{11}$  (dB), and antenna bandwidth.

#### 3. Antenna Design

This section provides a quick overview of the suggested technical design method for antennas. At a resonance frequency of 921 MHz, the antenna is created and modelled using Computer Simulation Technology (CST) Microwave Studio. A brief explanation of the technical and strategic approach for the suggested antenna is given. First, a standard reference antenna in the air scenario—a Rectangular Microstrip Patch Antenna (RMPA)—is used in the design process. The reference antenna is then a conventional rectangular patch. For comparison, a reference case for a square MPA manufactured on FR4 dielectric material is employed. The lower portion of this antenna also had a truncated ground plane. The rectangular patch antenna's impedance bandwidth is controlled by the truncated ground plane, which also serves as an impedance matching component.

In this study, the antenna configurations are printed on the FR4 epoxy substrate with a dielectric constant,  $\varepsilon_r = 4.3$ , a thickness, h = 1.60 mm, a metallization thickness of t = 0.035 mm at operating frequency,  $f_0$  of 921 MHz, whereas the speed of light,  $c = 3 \times 10^8$  m/s. The dimensions of the proposed RMPA have been calculated based on the proposed sets of design equations from the literature and optimised through a full parametric study. The obtained values for the parameter are illustrated in Table 1.

For the single patch rectangular element, the tentative length,  $L_p$  and width,  $W_p$  of the patch were calculated as 78.35 mm and 100.05 mm, respectively, for an operating frequency of 921 MHz by using rectangular patch design equations as stated in Table 1. However, to achieve the desired result of smaller dimensions, high gain and wider bandwidth, the parameters of the single patch element were drastically optimized to 75.5 mm  $\times$  90.6 mm ( $L_p \times W_p$ ). The thickness of the microstrip patch was 1.6 mm. The single patch element antenna was fed with a microstrip feedline,  $W_f$  of width 2.3 mm to achieve impedance matching. Matching

the input impedance of the antenna to 50  $\Omega$  is a prerequisite to ensuring that the maximum power is transferred.

	e 1. Dimensions of the prope		X7-1
Antenna Parameters	Formula		Values (mm)
Patch Width, W	$W = \frac{c}{2f_0\sqrt{\frac{\varepsilon_r + 1}{2}}}$	(1)	100.05
<b>Effective Dielectric</b>			
Constant, €eff	$ \varepsilon_{eff} = \frac{\varepsilon_r + 1}{2} + \frac{\varepsilon_r - 1}{2} \left( \frac{1}{\sqrt{1}} \right) $	$\frac{1}{1+12\frac{h}{W}}$ (2)	4.16
Effective Length, Leff	$L_{eff} = \frac{c}{2f_0\sqrt{\varepsilon_{eff}}}$	(3)	79.84
Patch Length	$0.412h(\varepsilon_{0.66}+0.3)(\frac{W}{2})$	$\frac{7}{1} + 0.264$	
Extension, $\Delta L$	$\Delta L = \frac{0.412h(\varepsilon_{eff} + 0.3)(\frac{W}{h})}{(\varepsilon_{eff} - 0.258)(\frac{W}{h})}$	+0.8 (4)	0.75
Patch Length, L	$L = L_{eff} - 2\Delta L$	(5)	78.34

The simulated result for return loss magnitude, S<sub>11</sub> (dB) and antenna bandwidth of the finalized single patch element antenna are shown in Figs. 1(a) and (b) respectively. The minimum value of the simulated on return loss, S<sub>11</sub> (dB) at the working frequency of 921 MHz is 22.67 dB. Meanwhile, the simulated bandwidth of a single patch element antenna is 20 MHz with a fractional bandwidth of 2.17%, which is not wide enough for underwater applications. The antenna performance parameters are listed in Table 2. Based on the data provided in Table 2, therefore, it is proven that some modifications to the single patch element antenna should be made in order to achieve the best results in antenna performance.

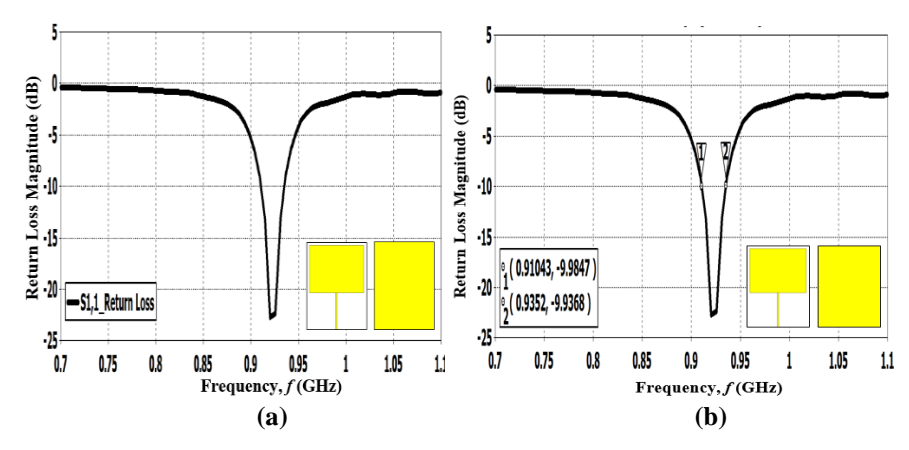


Fig. 1. Simulated results of (a) return loss and (b) bandwidth.

Table 2. The single patch element performance parameters.

Antenna	Freq	Return Loss	Area	$\mathbf{B}\mathbf{w}$	Gain
Туре	(MHz)	S <sub>11</sub> (dB)	$(mm^2)$	(MHz)	(dB)
Single Patch Element	921	-22.67	6840.30	20	-0.31

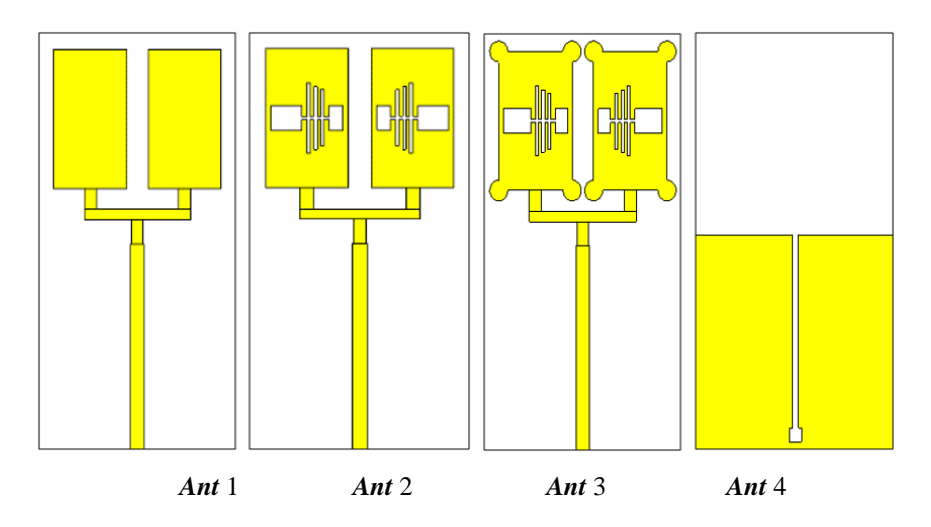
Due to the single patch element's failure to provide the desired antenna performance, an antenna array was created by connecting two single patches together via the combined corporate feed network. This is due to the fact that employing the idea of array design is one of the most popular ways to increase the gain of MPA.

#### Design evolution process of the proposed geometry of various antennas in air

Designing a compact underwater antenna faces a large number of difficulties. This is because, an efficient antenna is needed for underwater communications. Antenna performance is very important part to be considered while reducing the size of antenna. In order to miniaturize a RMPAAs, slots, rounded corner structures, and ground plane changes were all incorporated in this work.

In this design, a fishbone-shaped slot structure was included to examine the bandwidth's impact on the return loss  $S_{11}$  (dB). The compound slot structure, which has two main slots and subsidiary slots, is shaped like a fishbone. The head and tail pieces, which were separated into two sections from the main slots, are used to refer to these sections. On the two sides of the principal slots are the subsidiary slots, sometimes referred to as spines, which are positioned asymmetrically. The radiation pattern is stabilised, and total gain is increased by using rounded edges. Because it has been discovered in the literature to improve both the impedance bandwidth and the gain of the antenna, a rounded corner approach was thus adopted in this study [11]. To obtain the wide bandwidth, the proposed underwater antenna with a T-shaped slot has been introduced to enlarge the impedance bandwidth, besides having a simple structure and being easily implemented [12].

In this study, there are four steps have been taken to complete the intended antenna. In order to discover the optimal optimization during the simulations, four modified antennas were suggested. Only one of the four types of designs will be used to carry out this investigation. The final design's chosen dimensions are determined by the deeper resonance dips of S<sub>11</sub> (dB), tiny dimensions, improved gain, and return loss magnitude (in terms of dB). In Fig. 2, the evolution of the proposed antenna model is shown. Further discussion on Fig. 2, has been described in section 4.1.



**Journal of Engineering Science and Technology** 

April 2024, Vol. 19(2)

Fig. 2. Proposed geometry of various antennas involved in the design evolution.

#### 4. Results and Discussion

The creation of a small underwater antenna is fraught with several challenges. By changing one parameter while holding the others constant, the design antenna structure's varied dimensions were optimised. To achieve the best results, the critical parameters in the antenna design process should be optimised. Based on a number of factors, the antenna is examined. Knowing which variables have a significant impact on the characteristics and functionality of the proposed antenna during design is crucial for determining how well-matched an antenna is.

# 4.1. Antenna configurations in air

To maximise the performance of the four various types of RMPAAs, the evolution process is employed. By adjusting the antenna structure and optimising the dimensions, design optimization was carried out. The initial design, known as *Ant* 1, is a typical patch array antenna. The simulated result on return loss shown 36.6 dB while the bandwidth of *Ant* 1 depicted 300 MHz at the frequency of 904 MHz.

Then, a typical patch array antenna (*Ant* 1) and a fishbone-shaped slot structure (*Ant* 2) make up the second design. The results show that, the resonant frequency shifted from 904 MHz to 893 MHz. The simulated result exhibits the return loss of 38.9 dB and the bandwidth of 304 MHz which is better than *Ant* 1's result.

Afterward, the second design, *Ant* 2, is combined with *Ant* 3's rounded corner structures to create the third design. The simulated result on return loss yield a better result at 39.1 dB and the simulated bandwidth of this designed displays a broader bandwidth of 320 MHz.

To enhance the performance of the antenna in the final stages, an antenna was incorporated into the T-shaped slot structure at the substrate's back plane. In this configuration, this antenna is designated as *Ant* 4. As shown in Fig. 3, the curve displays a deep dip, where the return loss value is as low as 41.83 dB at 904 MHz. This antenna also exhibits a wider bandwidth of 295 MHz. As a consequence, the findings underline that the return loss is greatly affected by added the T-shaped slot structure.

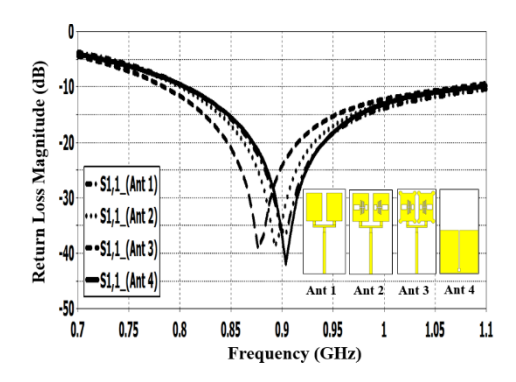


Fig. 3. Simulated results of return loss,  $S_{11}$  (dB) on different types of antenna configurations.

This result provided a good starting point for further investigation into the optimal conditions for reducing the antenna's size while enhancing its gain and bandwidth. In order to provide the required bandwidth and radiation sensitivity, the truncated ground plane was introduced at the back plane of each [13]. Figure 3 depicts a generic schematic for this technology's design architecture.

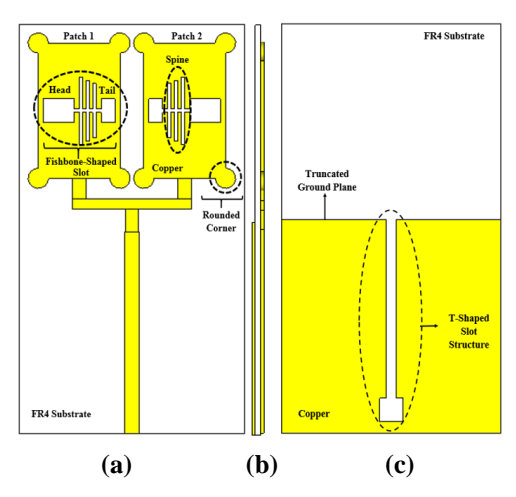
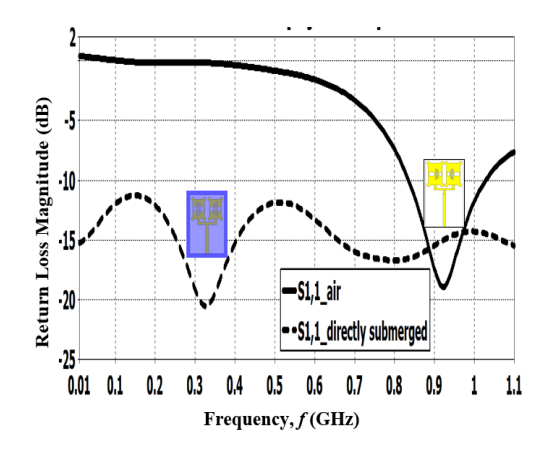


Fig. 4. Perspective schematic diagram and designed architecture (a) front view (b) left side view (c) rear view.

In this study, a waterproof barrier such as a plastic coating is needed to allow the propagation of electromagnetic wave. In Fig. 5, the resonant frequency moves from 921 MHz to 326 MHz as the simulated antenna in air condition was then simulated in underwater environment. The frequency shift of which is over 64.60%, indicating that the wavelength of an electromagnetic wave in freshwater will be significantly shorter than in the air. As illustrated in the plots, when the antenna is exposed to the air, the curve displays a deep dip, where the return loss value is as low as 18.93 dB at 921 MHz. However, if the antenna is surrounded by plastic coating, the S<sub>11</sub> parameter across different frequencies at 326 MHz and exhibits a better return loss of 20.49 dB. From this result, the parametric studies were performed to achieve the targeted performance of the proposed antenna in freshwater environment.



**Journal of Engineering Science and Technology** 

Fig. 5. Simulated results of return loss S<sub>11</sub> (dB) when the proposed antenna in air and directly submerged in freshwater.

#### 4.2. Parametric analysis of parameters in freshwater

This section explores in detail the affected parameters from the parametric studies as well as the performance of the proposed underwater antenna in a freshwater scenario. The optimization of various dimensions of the designed antenna structure was done by varying one parameter and fixing the others. Variation of several antenna parameters have significant effects on results and hence these points are taken into consideration while designing the antenna. In this study, the key parameters of the proposed antenna can be named as patch array dimensions ( $L_1$ ,  $W_1$ ), fishbone-shaped slot ( $L_2$ ,  $W_2$ ,  $L_3$ ,  $W_3$ ), rounded corner ( $R_c$ ), truncated ground plane ( $L_g$ ,  $W_g$ ), T-shaped slot for line length and width ( $L_{11}$ ,  $W_{11}$ ,  $L_{12}$ ,  $W_{12}$ ). The design, simulation and optimization processes of these parameters are performed in CST software. In CST, the parameters can be optimised by defining the upper and lower limits for each parameter.

There are four important parameters involved in forming the main slot's structure. But, here, the subsidiary slots (loading bars) are shown in Figs. 6 and 7, which includes the length parameter of  $L_4$ ,  $L_5$  and  $L_6$  and the width of parameter  $W_4$ ,  $W_5$  and  $W_6$  is not considered in the parametric analysis since the return loss magnitude,  $S_{11}$  (dB) showed small changes due to the limited space of the antenna design. Thus, all these parameters were not depicted here.

Slots was introduced to increase an effective length of the current path with the aim to miniaturize the antenna. The increment of current path increasing the effective capacitance, C and inductance, L of the design leading to a decrement in the resonant frequency of the antenna as derived from the Eq. (6) [14].

$$f_r = \frac{1}{2\pi\sqrt{LC}} \tag{6}$$

Based on the modelling parameters, there are several potential parameters that might make a major contribution to this research, which are the length of the main slots (head part),  $L_2$  and the width of main slots (head part),  $W_2$ . Varying the length of main slots (head part),  $L_2$  from 1.0 mm to 5.0 mm alters the  $S_{11}$  (dB). The increasing numbers for  $L_2$  parameter results the lower dip of  $S_{11}$  (dB) at 34.34 dB. The results show that an improvement in return loss,  $S_{11}$  (dB) characteristics can be easily obtained at  $L_2 = 5.0$  mm. Moreover, the parameter  $L_2$  resulted narrower bandwidth of 334 MHz as the parameter  $L_2$  increased, which cover the frequency from 754 MHz to 1088 MHz band.

Meanwhile, the parameter  $W_2$  displays a similar pattern as the parameter  $L_2$ . The width of the main slots (head part),  $W_2$  is varied from 1.0 mm to 3.0 mm by an interval of 1.0 mm while keeping the dimensions of parameter  $L_2$  and the rest of the parameters the same as in Table 3. The optimal value is obtained when parameter  $W_2$  equals to 3.0 mm with a return loss,  $S_{11}$  (dB) of 34.68 dB. In addition, the impedance bandwidth becomes narrower with the increment of  $W_2$ . When  $W_2$  is equal to 3.0 mm, it has a bandwidth of 332 MHz, which can cover the entire 753 MHz to 1086 MHz band.

A similar approach was followed for parameters  $L_3$  and  $W_3$ . The affected parameters of the designed antenna must be carefully considered to ensure the gain

is not affected while improving the return loss magnitude and bandwidth. It is clearly demonstrated that as the length of the main slots (tail part) increases,  $L_3$  increases from 1.0 mm to 5.0 mm, with the best optimization achieved when  $L_3$  is equal to 5.0 mm with a return loss of 33.80 dB. The wide bandwidth of 335 MHz is observed from 1090 MHz to 754 MHz.

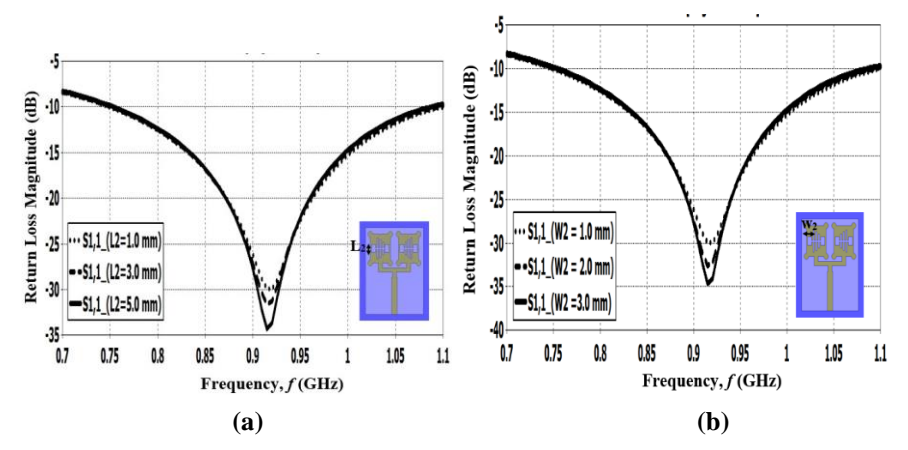


Fig. 6. Simulated results of varying parameter (a)  $L_2$  and (b)  $W_2$ .

In the meantime, from the simulated results of the width of the main slots (tail part),  $W_3$  the antenna has the better reflection coefficient at 3.0 mm. From the simulations of the width of  $W_3$ , it is concluded that, as the value of  $W_3$  increased, it was evident that the antenna started operating more effectively with respect to the  $S_{11}$  (dB). The parameter  $W_3$  had a bandwidth of 337 MHz and the return loss of 33.67 dB return loss.

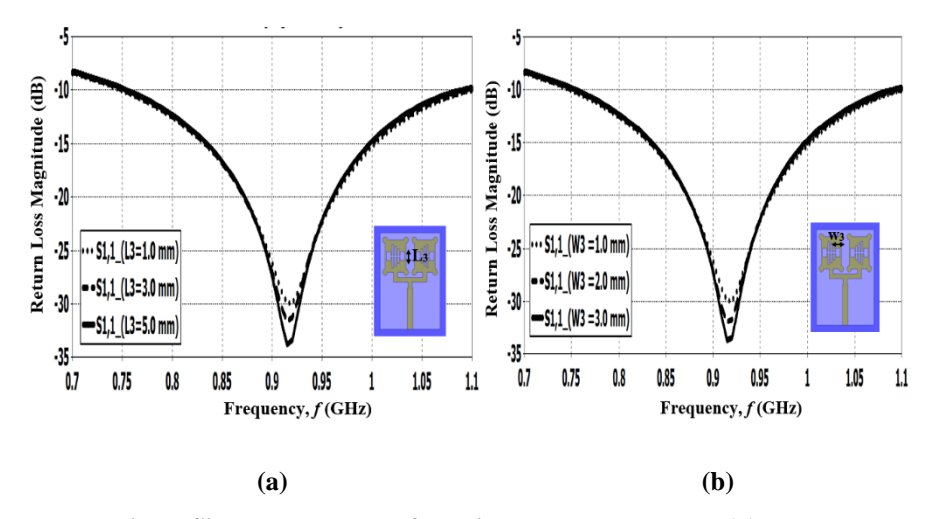


Fig. 7. Simulated results of varying parameter  $L_3$  and (b)  $W_3$ .

During the next step of the design process, the geometrical radius of the rounded corner,  $R_c$  of the proposed antenna was tuned to yield as much gain as possible. It is observed that, as the radius of rounded corner,  $R_c$  increases, the simulated design

produced a good impedance matching at 30.0 dB with a wide bandwidth of 350 MHz and also improved gain at -16.4 dBi. From the simulated results, the radius of rounded corner,  $R_c$  achieved the optimal value when  $R_c = 1.8$  mm.

Based on the design results obtained from Fig. 8(b), it is obvious that, by varying the length of the T-shaped slot structure,  $L_{11}$ , the resonant frequency is shifted to the left while reducing the bandwidth. The parameter value of  $L_{11} = 13.5$  mm is found to be the best compromise value for optimized return loss,  $S_{11}$  (dB) at 30.0 dB and the bandwidth achieved the optimal value of 351 MHz which cover the entire from 749 MHz to 1100 MHz. Meanwhile, as the parameter  $W_{11}$  is expanded the dimensions, the return loss,  $S_{11}$  (dB) showed a minor changes or has no effect on the performance of the antennas as the reflection coefficient results obtained are very similar. Thus, the result on return loss,  $S_{11}$  (dB) of this parameter was neglected since it does not affect too much.

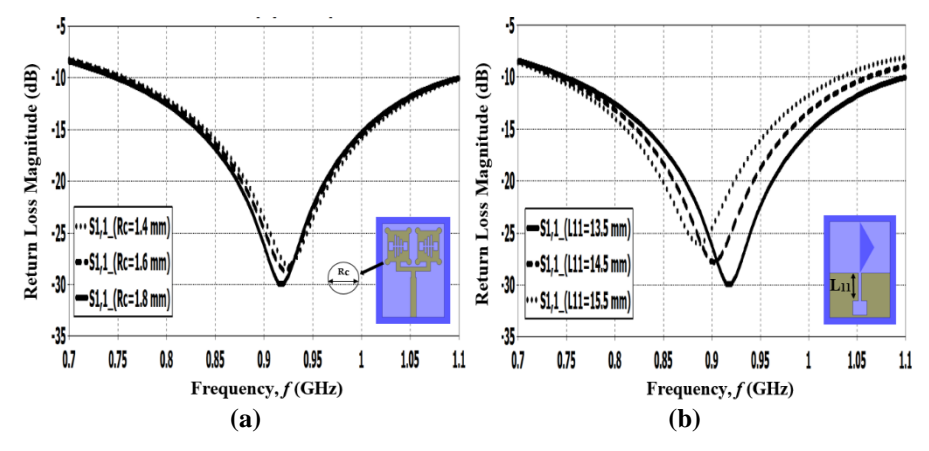


Fig. 8. Simulated results of varying parameter  $R_c$  and (b)  $L_{11}$ .

However, as can be seen from Fig. 9(a), as the parameter of  $L_{12}$  changes from 8.0 mm to 9.0 mm and 10.0 mm, respectively, the results of the return loss magnitude,  $S_{11}$  (dB) change dramatically and shift to the left side. Finally, it was found that the parameter  $L_{12}$  achieved the best results at  $L_{12}$  equal to 8.0 mm with the lowest return loss of 30.0 dB.

Similarly to the parameter  $W_{12}$ , it is found that, as the width of T-shaped slot structure,  $W_{12}$  increases from 10.0 mm to 11.0 mm by an interval of 0.5 mm, the parameter  $W_{12}$  suffers from a low return loss magnitude,  $S_{11}$  (dB) at 30.0 dB. Moreover, it is also found that, the parameter  $W_{12}$  is another important parameter that influences the bandwidth of the proposed design. Then, the optimal result from the simulated  $W_{12}$  parameter is found at 10.0 mm with the impedance bandwidth of 353 MHz.

The modified truncated ground plane acts as an impedance matching element to control the impedance bandwidth of a rectangular patch [15]. Therefore, as the height of the truncated ground plane structure,  $L_g$  increases, the results indicate that the impedance matching is increased and the frequency shifts to the left, but the gain of the proposed antenna is greatly reduced. Besides, modification to the ground plane increased the space between the rectangular patch and the ground, thereby cancelling out the inductive and capacitive effects [16]. Finally, it can be seen that

the stable length of the ground plane,  $L_g$  for this design is 25.0 mm. It means, the result is significantly affected by adjusting the length to achieve the impedance matching. The return loss magnitude,  $S_{11}(dB)$  of the antenna improves dramatically at 29.96 dB when the length of the ground patch reduces gradually, and the best result is obtained at the height of the ground plane,  $L_g$  of 25.0 mm.

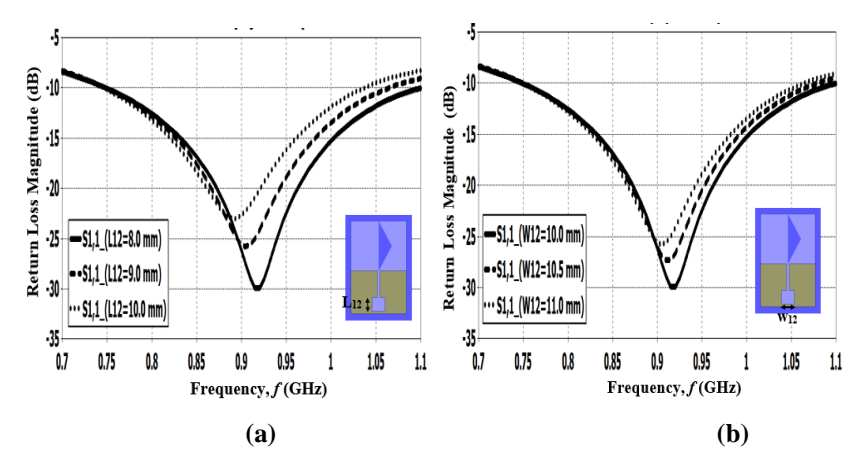


Fig. 9. Simulated results of varying parameter (a)  $L_{12}$  and (b)  $W_{12}$ .

From the graph obtained in Fig. 10(b), it is seen that by changing the ground plane width,  $W_g$  has shown a significant effect on the impedance matching. The width of the ground plane,  $W_g$  achieved the best optimal value at 43.0 mm with return loss of 29.96 dB. It was found that the ground plane has a critical impact on the antenna's performance, and it is one of the main challenges in minimizing antenna size [17]. Both of the parameters  $L_g$  and  $W_g$  achieved the same bandwidth at 353 MHz.

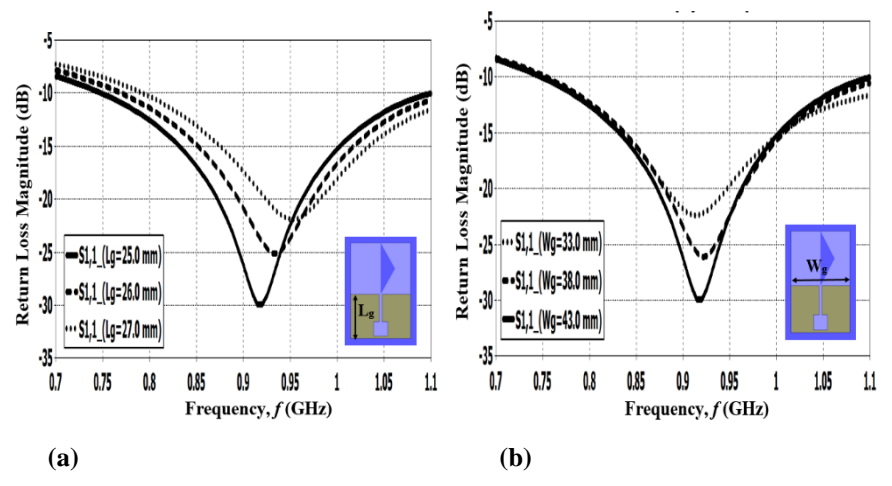


Fig. 10. Simulated results of varying parameter (a)  $L_g$  and (b)  $W_g$ .

# 4.3. Antenna dimension and optimization

After the parametric studies in the simulation process were finished successfully, the optimal shape of the proposed underwater antenna was found based on the expected frequency band [18]. The schematic design of the proposed underwater antenna is demonstrated in Fig. 11, including its optimised dimensions. From the figure shown, it is clearly depicted that the separation between the top and bottom planes of the substrate. The two elements of the rectangular patch array antenna were separated by the distance, which was denoted as d. The overall dimensions of the proposed underwater antenna are  $54 \times 43$  mm<sup>2</sup>, which corresponds to  $0.16 \, \lambda_o \times 0.13 \, \lambda_o$ , where  $\lambda_o$  is the operating wavelength. Moreover, a partial ground plane has a size of  $25.0 \times 43.0$  mm<sup>2</sup>.

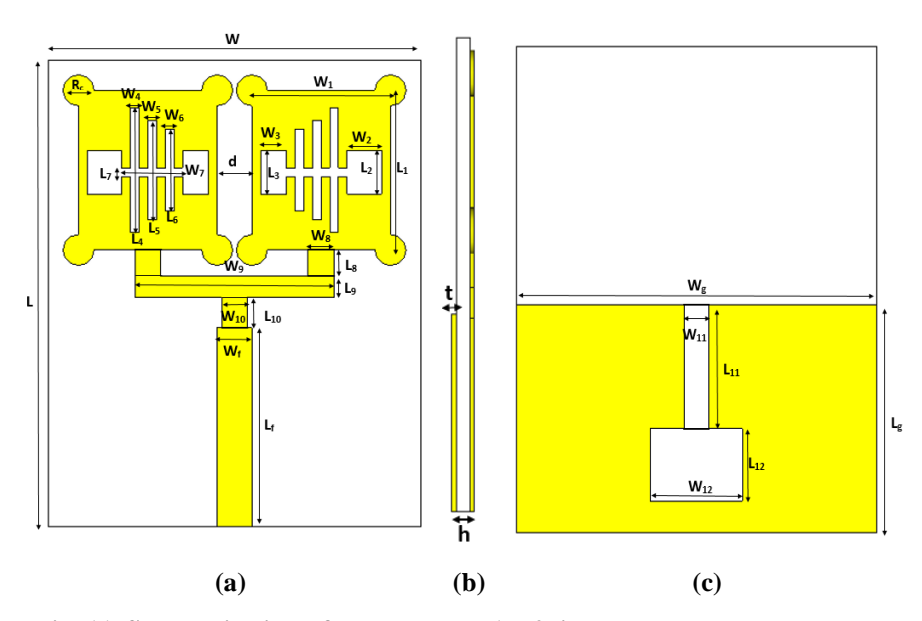


Fig. 11. Schematic view of the proposed  $1 \times 2$  linear rectangular patch array antenna in freshwater scenario (a) front view (b) left side view (c) rear view

Table 3. Dimensions of	f the proposed
antenna in freshwater (Ta	p Water) scenario.
T7 1	- n 4

Parameter	Value	Parameter	Value
Relative Permittivity, $\varepsilon_r$	78	$L_2 \times W_2$	$5.0 \times 3.0 \text{ mm}^2$
Electrical Conductivity, σ	1.59 S/m	$L_3 \times W_3$	$5.0 \times 3.0 \text{ mm}^2$
Thickness of Copper, t	0.035 mm	$L_4 \times W_4$	$13.0\times1.0~mm^2$
Substrate $(L \times W \times h)$	$54.0\times43.0\times1.6~mm^3$	$L_5  imes W_5$	$10.0\times1.0~\text{mm}^2$
Patch $(L_1 \times W_1)$	$18.0 \times 15.0 \text{ mm}^2$	$L_6 \times W_6$	$8.0 \times 1.0 \text{ mm}^2$
Strip Line $(L_{10} \times W_{10})$	$3.0 \times 3.0 \text{ mm}^2$	$L_7  imes W_7$	$1.0\times7.0~\text{mm}^2$
Feeding Line $(L_f \times W_f)$	$3.5 \times 3.0 \text{ mm}^2$	$L_8 \times W_8$	$3.0 \times 3.0 \text{ mm}^2$
Ground Plane $(L_g \times W_g)$	$25.0 \times 43.0 \text{ mm}^2$	$L_9 \times W_9$	$2.5\times24.0~\text{mm}^2$
Rounded Corner, $R_c$	Diameter – 3 mm	$L_{11} \times W_{11}$	$13.5\times2.0~\text{mm}^2$
Distance between Patch	d - 1.8  mm	$L_{12} \times W_{12}$	$8.0\times10.0~\text{mm}^2$

### 4.4. Feeding technique and T-junction power divider

A power divider is needed to connect the two elements of the microstrip antenna array with a transmission line, which generally has a 50  $\Omega$  impedance. T-Junction

**Journal of Engineering Science and Technology** 

is a method to connect the two patch microstrip antenna as a radiating element arranged in a row (corporate feed). To calculate both impedance matching can be obtained using Eq. (7) [19]

$$Z = Z_0 \times \sqrt{N} \tag{7}$$

where Z is the required impedance value according to the number of microstrip antenna element arrays,  $Z_0$  is the input impedance of the microstrip ( $Z_{in}$ ) antenna, and N is the number of elements or arrays of microstrip antennas. From Eq. (8) the value of required impedance for two elements can be obtained. If  $Z_0 = 50 \Omega$ , and the number of patch element N = 2, then the value of impedance Z is equal to

$$Z = 50 \times \sqrt{2} = 70.71 = 70.7 \,\Omega \tag{8}$$

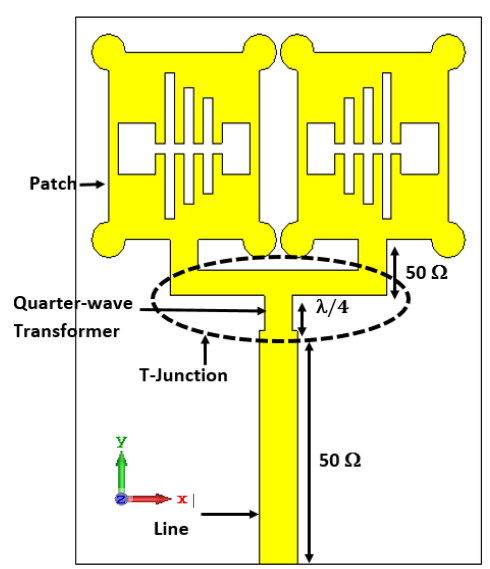


Fig. 12. The schematic diagram of two elements array line impedance design layout.

# 5. Methodology of Experiments

To evaluate and validate the antenna characteristics in a freshwater environment, a series of measurements were made. A prototype that is depicted in Fig. 13(b) was created and experimentally studied. The proposed underwater antenna was then encapsulated within the plastic to make it waterproof. This is necessary to offer strength and strain relief, as well as to prevent water entry, which might corrode the rectangular patch array connectors and metal components of the coaxial cable.

#### **5.1.** Measurement setup in the laboratory (Freshwater Scenario)

The suggested antenna was tested in an experiment inside a rectangular glass tank filled with tap water. The Keysight Power Network Analyzer, PNA, model N5227A, test port cable and proposed antenna were then joined. Figure 13(a) depicts the measurement setup for the suggested antenna in an underwater environment, and Fig. 13(b) shows a picture of the prototype antenna. A measurement was made using a freshwater sample from the type of tap water. The

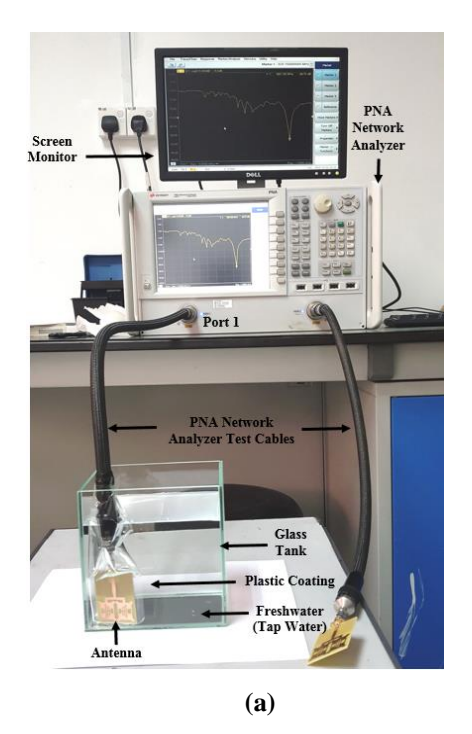
importance of fully submerging the antenna in water has been emphasised for future analysis of the antenna bandwidth and return loss magnitude,  $S_{11}$  (dB).

# 5.2. The results of simulated and measured of return loss, $S_{11}\left(dB\right)$ and bandwidth

The design principle of the suggested underwater antenna has been carried out by following four steps in the radiating microstrip patch array without any change in the partial ground structure. However, the difference in this study is, the proposed design will be simulated in normal water with a permittivity of 78 with electrical conductivity of 1.59 S/m and the ambient temperature of 25°C will be used as a propagation medium. The properties of freshwater is shown in Table 4.

Table 4. Properties of freshwater (Normal Water).

-	
Parameters	Value
Relative Permittivity, $\varepsilon_r$	78
Permeability	0.999991
Electrical Conductivity, $\sigma$	1.59 S/m
Density	$1000 \text{ kg/m}^3$
Thermal Conductivity	0.6 W/K/m
Heat Capacity	4.2 kJ/K/kg
Diffusivity	$1.42857 \times 10^{-7} \text{ m}^2/\text{s}$



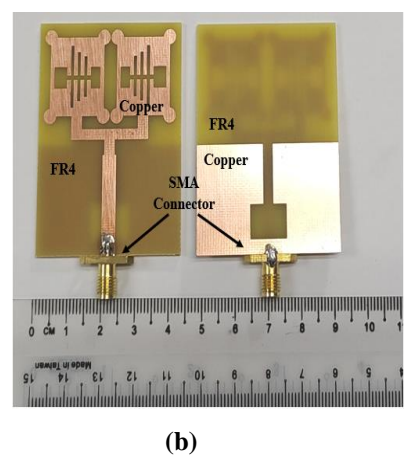


Fig. 13. (a) Measurement setup of the proposed antenna in freshwater scenario (b) Photograph of the fabricated antenna (front and back plane)

This section will first give the suggested antenna's return loss magnitude,  $S_{11}$  (dB), and bandwidth data in order to further enlighten the study. Figure 14

**Journal of Engineering Science and Technology** 

compares the simulation and observed results for the size of the return loss, S<sub>11</sub> (dB), as a function of operating frequency. The measured return loss magnitude at the same resonant frequency was equal to 28.69 dB, while the simulated return loss obtained is equivalent to 30.0 dB. According to Fig. 12, the measured and simulated antenna bandwidths, which ranged from 870.0 MHz to 980.0 MHz, and 700.0 MHz to 1100.0 MHz, respectively, were estimated to be around 12% and 43.4%, respectively. All the results data obtained from the simulated and measured of the proposed antenna in freshwater (tap water) scenario has been tabulated in Table 5.

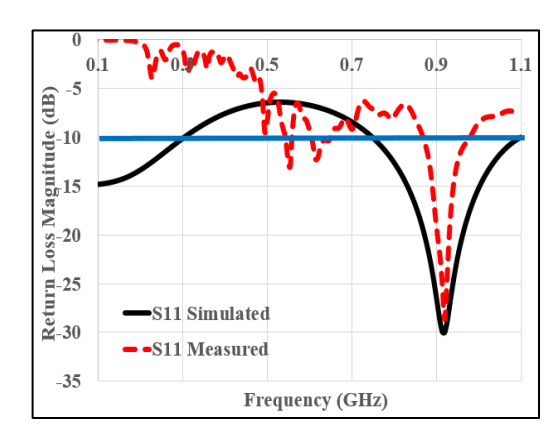


Fig. 14. Return loss magnitude,  $S_{11}\left(dB\right)$  for simulated and measured results in freshwater scenario

Table 5. Simulated and measured parameters in freshwater scenario.

Characteristics	Simulated	Measured
Frequency (MHz)	921	921
Return Loss Magnitude (dB)	-30.0 dB	-28.69 dB
Bandwidth (MHz)	700 to 1100 MHz	870 to 980 MHz
Fractional Bandwidth, FBW (%)	43.4%	12.0%

The mismatch between the results of simulation and fabrication is the most common significant error in this research. As expected, some minor differences were observed between the simulation and the measurement results, as in many published works of literature. The incompatibility between measurement and simulation is predominantly due to fabrication faults in the antenna design. Moreover, the slight discrepancy between them may be attributed to the fact that the presence of the SubMiniature Version A (SMA) connector only slightly degrades the impedance matching and shifts the resonant frequency. Besides, it can be due to attenuation through cable loss or as a result of reflection from the wall of the freshwater tank.

# 5.3. Simulated radiation pattern

The results of the simulated radiation patterns of the proposed antenna on the cutting planes  $\phi = 0^{\circ}$  (E-plane) and  $\phi = 90^{\circ}$  (H-plane) are presented and briefly discussed. Figures 15 (a) and (b) illustrate the simulated radiation patterns in the y-z and x-z planes at the centre frequency of 921 MHz.

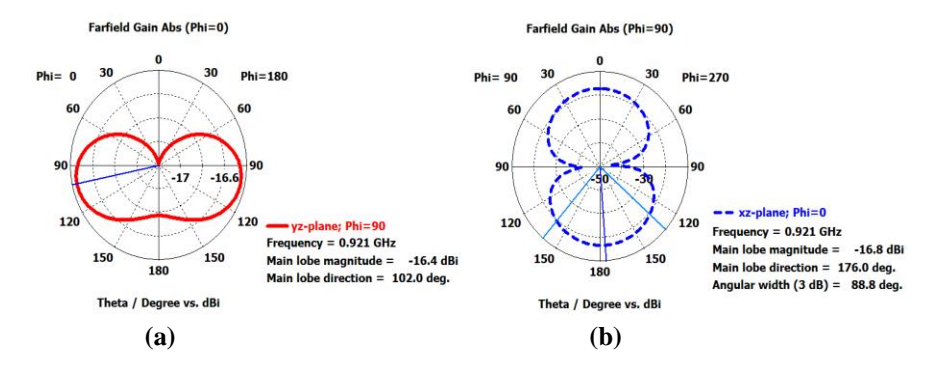


Fig. 15. Simulated radiation pattern of the proposed antenna (a) E-plane (b) H-plane radiation pattern.

#### 5.4. Simulated and measured gain

From the simulated results, the gain of the proposed antenna operating in freshwater (tap water) exhibits the maximum gain of -16.4 dBi as shown in Fig. 16.

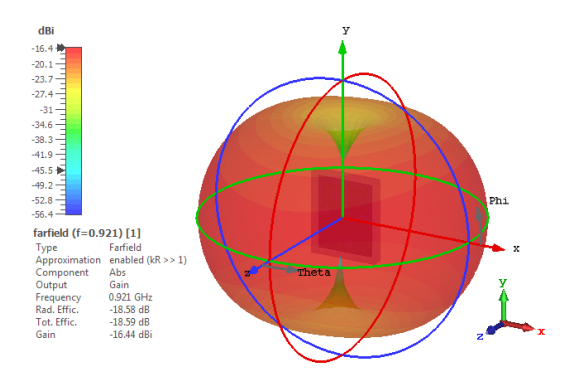


Fig. 16. Simulated gain of the proposed underwater antenna.

Measuring the gain of an antenna accurately is a very challenging task and is most commonly performed in an environment with non-reflecting characteristics like in an anechoic chamber or an open test site. The Friis Transmission equation is used to determine the gain of the antenna using the measured transferred power as shown in:

$$Z\frac{P_r}{P_t} = \left(\frac{\lambda}{4\pi R}\right)^2 G_t G_r \tag{9}$$

where  $G_t = G_r = G$  and  $G_t$  is the gain of transmitting antenna and  $G_r$  is the gain of receiving antenna.

This equation can be re-written in terms of dB as:

$$G_{dB} = \frac{1}{2} \left[ 20 \log_{10} \left( \frac{4\pi R}{\lambda} \right) + 10 \log_{10} \left( \frac{P_r}{P_t} \right) \right]$$
FSPL
$$S_{21}$$
(10)

**Journal of Engineering Science and Technology** 

where  $G_{db}$  is the gain of antenna under test (AUT) in dB, R is the distance between two antennas,  $P_t$  is the transmitted power,  $P_r$  is the received power,  $\lambda$  is the wavelength and FSPL is the free space path loss propagation. The  $S_{21}$  recorded by the spectrum analyser and the accurate distance between the antennas will provide the gain of the antenna using Eq. (9).

$$G_{dB} = \frac{1}{2} \left[ 20 \log_{10} \left( \frac{4\pi (25 \times 10^{-3})}{\frac{3 \times 10^{8}}{921 \times 10^{6}}} \right) + (-23.31 \text{ dB}) \right]$$
 (11)

$$G_{dB} = \frac{1}{2} [18.77 \text{ dB} - 23.31 \text{dB}] = -2.27 \text{ dB}$$

#### 6. EM Wave Propagation in Freshwater

Freshwater is a low-loss medium due to its low conductivity [5]. The propagation speed can be expressed as

$$c \approx \frac{1}{\sqrt{\varepsilon \mu}} \tag{12}$$

where  $\varepsilon$  is dielectric permittivity and  $\mu$  is magnetic permeability. The dielectric permittivity can be expressed as a product of the permittivity in air,  $\varepsilon_0 = 8.854 \times 10^{-12}$  and the dimensionless relative permittivity,  $\varepsilon_r = 78$ . Since water is a non-magnetic medium, the value of its relative permeability is  $\mu_r = 1$ , the permeability,  $\mu$  of the water is the same permeability as that of free space,  $\mu_0$ 

$$c \approx \frac{1}{\sqrt{\varepsilon_0 \varepsilon_r \mu_0 \mu_r}} = \frac{1}{\sqrt{8.854 \times 10^{-12} \times 78 \times 4\pi \times 10^{-7} \times 1}}$$

$$c \approx 33.95 \times 10^6 \text{ m/s}$$
(13)

The main factor of attenuation in the RF underwater channel is the absorption loss. Therefore, the absorption coefficient,  $\alpha_{fw}$  for freshwater is given as:

$$\alpha_{fw} = \frac{\sigma}{2} \sqrt{\frac{\mu}{\varepsilon}} \tag{14}$$

where  $\varepsilon$  is dielectric permittivity and  $\mu$  is magnetic permeability

$$\alpha_{fw} = \frac{\sigma}{2} \sqrt{\frac{\mu_0 \mu_r}{\varepsilon_0 \varepsilon_r}} = \frac{1.59}{2} \sqrt{\frac{4\pi \times 10^{-7} \times 1}{8.854 \times 10^{-12} \times 78}} = 33.91 \text{ Np/m}$$
 (15)

## 7. Conclusions

A fully underwater antenna is described in this article along with a thorough explanation of the design, simulation, and fabrication method. With a permittivity of 78 and an electrical conductivity of 1.59 S/m, this work primarily focused on antenna design for standard underwater communications. In this paper, a parametric analysis of important dimensions was also performed. Prototype antennas have been made and measured. To do this, a theoretical analysis that took into consideration the technical aspects of the electromagnetic propagation was conducted to ascertain the actual viability of this underwater communication. The theoretical analysis has been well supported by experimental findings. The importance of ideal antenna characteristics, such as a straightforward structure,

simple manufacture, low price, small size, and light weight, has also been highlighted. As a result, this research on the suggested antenna has shown that it is possible to develop an underwater EM communication system with a large communication range without compromising other performance metrics.

Nomencla	Nomenclatures		
Tiomenera	icui es		
c	The speed of light, $c = 3 \times 10^8 \text{ m/s}$		
$f_0$	Operating frequency, MHz		
$G_{dB}$	Gain of antenna under test (AUT), dB		
$G_r$	Gain of receiving antenna, dB		
$G_t$	Gain of transmitting antenna, dB		
h	Thickness of substrate, mm		
L	Patch length, mm		
$L_{ m eff}$	Effective length, mm		
$P_r$	Received power, W		
$P_t$	Transmitted power, W		
R	Distance between two antennas, mm		
t	Thickness of metallization, mm		
W	Patch width, mm		
Greek Sym	bols		
$lpha_{ m fw}$	Absorption coefficient in freshwater		
$\Delta L$	The extended length of patch antenna, mm		
$\varepsilon$	Dielectric permittivity, F/m		
<b>E</b> 0	Permittivity in air, F/m		
$\mathcal{E}_{ ext{eff}}$	Effective dielectric constant		
$\mathcal{E}_r$	Relative permittivity		
λ	Wavelength, mm		
μ	Magnetic permeability, H/m		
$\mu_0$	Permeability in air ≈ 1		
$\mu_r$	Relative permeability		
$\sigma$	Electrical conductivity, S/m		
Abbreviati	•		
AUT	Antenna Under Test		
CST	Computer Simulation Technology		
EM	Electromagnetic		
FR4	Flame Retardant 4		
FSPL	Free Space Path Loss		
LoRa	Long Range		
MHz	Megahertz		
MPA	Microstrip Patch Antenna		
PIFA PNA	Planar Inverted F Antenna Power Network Analyzer		
RMPA	Power Network Analyzer Rectangular Microstrip Patch Antenna		
RMPAAs	Rectangular Microstrip Patch Array Antennas		
SMA	SubMiniature Version A		
SIVIA	Subivilliature version A		

#### References

- 1. Mokhtar, N.H.M.; Malek, N.A.; Jusoh, A.Z.; Ali, K.; Isa, F.M.N.; and Rahman, F.D.A. (2019). Design and comparison of printed antennas using meander line technique. *Bulletin of Electrical Engineering and Informatics*, 8(2), 596-603.
- Fidaus, M.R.; Herdiana, B.; and Iskandar, R.M. (2022). Modelling of antenna open half lamda using automatic antenna plotter detector testing at UHF broadcast frequency. *Journal of Engineering Science and Technology*, 17(5), 3099-3108.
- 3. Rakholiya, A.A.; and Langhnoja, N.V. (2017). A review on miniaturization techniques for microstrip patch antenna. *International Journal of Advance Research and Innovative Ideas in Education*, 3(2), 4281-4287.
- 4. Rambe, A.H.; Muharry, H.; Harahap, R.; and Suherman, S. (2018). Miniaturization of rectangular patch microstrip antenna by using complementary split ring resonator. *IOP Conference Series: Materials Science and Engineering*, 420, 012132.
- 5. Qureshi, U.M.; Shaikh, F.K.; Aziz, Z.; Shah, S.M.Z.S.; Sheikh, A.A.; Felemban, E.; and Qaisar, S.B. (2016). RF path and absorption loss estimation for underwater wireless sensor networks in different water environments. *Sensors*, 16(6), 890, 1-15.
- Abdou, A.A.; Shaw, A.; Mason, A.; Al-Shamma'a, A.; Cullen, J.; Wylie, S.; and Diallo, M. (2013). A matched bow-tie antenna at 433MHz for use in underwater wireless sensor networks. *Journal of Physics: Conference series*, 450, 012048.
- 7. O'Keefe, S.G.; and Perhirin, S. (2014). A passive auto-switching amphibian antenna. *IEEE Transactions on Antennas and Propagation*, 62(6), 3389-3392.
- 8. Mohd Zali, H.; Ibrahim, I.P.; Ali, M.T.; and Mahmood, M.K.A. (2019). Wideband microstrip antenna integrated with optimized buffer layer parameters for underwater wireless communication. *Journal of Electrical and Electronic Systems Research (JEESR)*, 15(12), 75-81.
- 9. Dala, A.; and Arslan, T. (2021). Design, implementation, and measurement procedure of underwater and water surface antenna for Lora communication. *Sensors*, 21(4), 133, 1-17.
- Jaafar, A.N.; Ja'afar, H.; Yamada, Y.; Sadeghikia, F.; Ibrahim, I.P.; and Mahmood, M.K.A. (2023). Design of an axial mode helical antenna with buffer layer for underwater applications. *International Journal of Electrical & Computer Engineering*, 13(1), 473-482.
- 11. Awais, Q.; Chattha, H.T.; Jamil, M.; Jin, Y.; Tahir, F.A.; and Rehman, M.U.(2018). A novel dual ultrawideband CPW-fed printed antenna for Internet of Things (IoT) applications. *Wireless Communications and Mobile Computing*, Volume 2018, Article ID 2179571, 1-9.
- 12. Wen, D.-L.; and Hao, Y. (2016). A wideband T-shaped slot antenna and its MIMO application. *Proceedings of the 2016 IEEE International Symposium on Antennas and Propagation (APSURSI)*, Fajardo, PR, USA, 1761-1762.
- 13. Ullah, S.; Ahmad, S.; Khan, B.A.; and Flint, J.A. (2018). A multi-band switchable antenna for Wi-Fi, 3G advanced, WiMAX, and WLAN wireless

- applications. *International Journal of Microwave and Wireless Technologies*, 10(8), 991-997.
- Ripin, N.; Sulaiman, A.A.; Rashid, N.E.A.; Hussin, M.F.; and Ismail, N.N. (2017). A miniaturized 878 MHz slotted meander line monopole antenna. Indonesian Journal of Electrical Engineering and Computer Science, 7(1), 170-177.
- 15. Karwa, M.; and Mathur, A. (2015). Rectangular microstrip patch antenna with truncated ground for ultra wide band. *International Journal of Engineering Research and General Science*, 3(2), 787-795.
- Kumar, O.P.; Ali, T.; and Kumar, P. (2023). A novel corner etched rectangular shaped ultrawideband antenna loaded with truncated ground plane for microwave imaging. Wireless Personal Communications, 130(3), 2241-2259.
- 17. Nassar, I.T.; and Weller, T.M. (2011). The ground plane effect of a small meandered line antenna. *Proceedings of the WAMICON* 2011 *Conference*, Clearwater Beach, FL, USA, 1-5.
- Ahsan, M.R.; Islam, M.T.; Habib Ullah, M.; Arshad, H.; and Mansor, M.F. (2014). Low-cost dielectric substrate for designing low profile multiband monopole microstrip antenna. *The Scientific World Journal*, Volume 2014, Article ID 183741, 1-10.
- 19. Sotyohadi, S., Somawirata, I.K., Widodo, K.A., Phung, S.T., and Zekker, I. (2021). Design and simulation "Ha"-slot patch array microstrip antenna for WLAN 2.4 GHz. *Proceedings of the Pakistan Academy of Sciences: A. Physical and Computational Sciences*, Pakistan, 109-117.